Advances in Seabed Liquefaction and Its Implications for Marine Structures

B. Mutlu Sumer[1]
[1] *Technical University of Denmark, DTU Mekanik, Section for Fluid Mechanics*
Coastal and Maritime Engineering, Kgs. Lyngby, Denmark
E-mail: bms@mek.dtu.dk

ABSTRACT: A review is presented of recent advances in seabed liquefaction and its implications for marine structures. The review is organized in seven sections: Residual liquefaction, including the sequence of liquefaction, mathematical modelling, centrifuge modelling and comparison with standard wave-flume results; Momentary liquefaction; Floatation of buried pipelines; Sinking of pipelines and marine objects; Liquefaction at gravity structures; Stability of rock berms in liquefied soils; and Impact of seismic-induced liquefaction.

KEYWORDS: Liquefaction, Waves, Marine structures, Seabed

1. INTRODUCTION

Seabed liquefaction is one of the important topics of marine hydro-geomechanics. In geotechnics, liquefaction refers to the state of the soil in which the effective stresses between individual soil grains vanish, and therefore the water-sediment mixture as a whole acts like a liquid. Under this condition, the soil fails, precipitating failure of the supported structure such as pipelines, sea outfalls, breakwaters, seawalls, pile structures, gravity structures, rock berms, and others.

Soil liquefaction caused by earthquakes has been studied quite extensively in the past thirty years or so. This has culminated into a substantial body of literature, including books by Seed and Idriss (1982), Kramer (1996, Chapter 9), and most recently, Jefferies and Been (2006) and Idriss and Boulanger (2008). Soil liquefaction caused by earthquakes with regard to its application for port structures is covered in a book "Seismic Design Guidelines for Port Structures", published by PIANC (The World Association for Waterborne Transport Infrastructure) in 2001 (PIANC, 2001). However, until recently, comparatively little has been known about the impact of liquefaction induced by water waves. Indeed, the topic has received little coverage in research, which has substantially advanced the design of marine structures but not the design of their foundations with regard to soil liquefaction. The European Union supported a three-year (2001-2004) research program on liquefaction around marine structures (LIMAS), which was preceded by another EU research program (1997-2000) on scour around coastal structures (SCARCOST) in which liquefaction around coastal structures was one of the focus areas. The main results of LIMAS were published in two special-issue volumes in Journal of Waterway, Port, Coastal and Ocean Engineering, American Society of Civil Engineers (ASCE) (see the editorials by Sumer 2006 and 2007), and those from SCARCOST were summarized in Sumer *et al*. (2001). The topic has continued to receive much attention, which has lead to a substantial amount of recent publications in journals and conference proceedings. A state-of-the-art knowledge based on the existing work has been collected in two recent books, Jeng (2013) and Sumer (2014).

The purpose of the present paper is to cover (partially) the recent work on wave-induced seabed liquefaction around marine structures with special emphasize on residual liquefaction; momentary liquefaction; floatation of buried pipelines; sinking of pipelines and marine objects; liquefaction at gravity structures; and stability of rock berms in liquefied soils. A brief account is also included of the seismic-induced seabed liquefaction and its impact. The present review is by no means exhaustive, probably biased with the author's own current research interest.

2. RESIDUAL LIQUEFACTION

2.1 Sequence of liquefaction

The sequence of liquefaction process has been studied by Miyamoto et al. (2004) and Sumer et al. (2004, 2006 a), two studies conducted independently from each other. Miyamoto et al. (2004), a theoretical and experimental investigation of liquefaction and solidification (of liquefied sand) during wave loading, did their experiments in a very small wave tank in a centrifuge, while Sumer et al. (2004, 2006 a) did their experiments in a standard wave flume. It was shown in Sumer et al. (2006 a) that their findings appear to be in agreement with the sequence of sediment behaviour reported in Miyamoto et al. (2004). The process typically has the following sequence: (1) With the introduction of the waves, the pore-water pressure (in excess of the static pore-water pressure) begins to build up; (2) When the built-up pore-water pressure reaches a critical value, the soil will liquefy, termed the onset of liquefaction; (3) The onset of liquefaction first occurs at the surface of the bed, and rapidly spreads out across the soil depth, reaching the impermeable bed, enabling the entire soil to act as a liquid (a mixture of soil and water); (4) In the liquefaction stage, the water and the liquefied soil form a two-layered system of liquids of different density, and the interface between the layers of this system will experience an internal wave; (5) With the arrival of the liquefaction front at the impermeable base, a new stage of the liquefaction sequence begins at the impermeable base, termed the compaction or solidification, in which the soil grains fall out of liquid state, settling through the water until they begin to come into contact with each other (This process somewhat resembles self-weight consolidation of hydraulic fill, see the discussion in Sumer, 2014, Chapter 3.); (6) Subsequently, the compaction gradually progresses in the upward direction, and the entire sequence of liquefaction/compaction process comes to an end when the compaction front arrives at the surface of the compacted soil. The final stage of the liquefaction process is the formation of sand ripples on the bed surface, as revealed by Sumer et al.'s (2006 a) wave flume experiments. The latter stage was not observable in Miyamoto et al.'s (2004) experiments.

Much work has been done in the past on various aspects of the liquefaction sequence. Recent reviews can be found in the books of Jeng (2013) and Sumer (2014). One of the much debated issues is the criterion for the onset of liquefaction. As mentioned in item 2 in the above description, the soil will liquefy when the accumulated pore-water pressure reaches a critical value, p_{cr}. The question has been whether p_{cr} is the initial vertical effective stress:

$$\sigma_{v0}' = \gamma' z \qquad (1)$$

or, the initial mean normal effective stress:

$$\sigma_0' = \frac{1}{3}(\gamma' z + k_0\gamma' z + k_0\gamma' z) = \gamma' z \frac{1+2k_0}{3} \qquad (2)$$

in which z is the depth measured from the surface of the seabed downwards (the mudline), γ' the submerged specific weight of the soil ($\gamma' = \gamma_t - \gamma$), γ being the specific weight of water, k_0 the coefficient of lateral earth pressure (or the lateral stress ratio) at rest. Sumer et al.'s (2012) measurements of pore-water pressure synchronized with video recording of the process have shown that the onset of liquefaction is associated with the initial mean normal effective stress, σ_0'. Namely, liquefaction occurs when $\overline{p}$ reaches σ_0' in which $\overline{p}$ is the accumulated period-averaged pore-water pressure. The topic has been discussed in detail in Sumer (2014, Section 3.1.2).

2.2 Mathematical modelling

Mathematical models have been developed to describe various stages of the liquefaction sequence. Of these, the models describing the buildup of pore pressure is essentially used to make assessments of liquefaction potential. Given the wave parameters, and the soil properties, these models predict the time series of the buildup of pore-water pressure, and the liquefaction risk is checked whether $\overline{p} > \sigma_0'$, the risk of liquefaction potential.

One such model has been described in Sumer et al. (2012): Sumer and Cheng (1999) developed an analytical solution for the differential equation which governs the buildup of pore water pressure. Their solution includes the periodic shear stress generated in the soil by a progressive wave. Hsu and Jeng (1994) produced an analytical solution for the latter quantity, solving the Biot equations. The mathematical model described in Sumer et al. (2012) essentially combines Sumer and Cheng's (1999) solution for the buildup of pore water pressure, and Hsu and Jeng's (1994) solution for the shear stress in the soil, and was first published in the book of Sumer and Fredsøe (2002). The model was later tested and validated against experiments in a series of controlled tests carried out in Sumer et al. (2012). A numerical example is also included in the latter publication to demonstrate the implementation of the model for real life scenarios. Figure 1 displays the result of the numerical example, illustrating the time development of the accumulated pore-water pressure under a progressive wave with a wave height of 6 m (see Sumer et al., 2012, for the soil properties and wave conditions); as seen, the accumulated pressure exceeds the value of the initial mean normal effective stress within less than 15 minutes, the onset of liquefaction. It may be noted that the same example indicates that no liquefaction occurs when the wave height is reduced to 5 m.

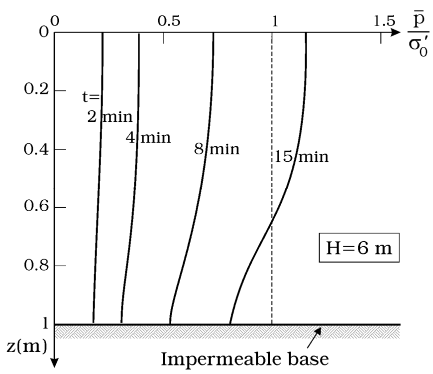

Figure 1 Time development of the accumulated pore pressure.

Seed and Rahman (1978) were the first to adopt the differential equation which governs the buildup of pore water pressure, the same equation as that used in Sumer et al. (2012). Spierenburg (1987) and McDougal et al. (1989) have subsequently adopted similar approaches. The works by Barends and Calle (1985) and de Groot et al. (1991) have considered similar theoretical descriptions of the process of pressure accumulation in the soil. Sekiguchi et al.'s (1995) study, on the other hand, focused on the generation of the pore pressure. Their poro-elastoplastic formulation enabled the researchers to obtain closed-form solutions for the accumulated pore pressure under cycling loading. Jeng et al. (2007) studied the effect of nonlinear mechanism of pore pressure generation on the buildup of pore pressure. Although the mechanism of pore pressure buildup and the nonlinear relation of pore pressure generation appear to be more important under larger wave, longer wave period and shallower water depth, the linear and nonlinear results apparently practically coincide for the accumulated pore pressure values $\overline{p}/\sigma_0'$ larger than O(0.1), the pressure values most important for practical applications. See discussion in Sumer (2014, Example 5).

The model described in Sumer et al. (2012) is for the general case with a finite soil depth. For the special case where the soil depth is infinitely large, Sumer and Fredsøe (2002) developed another analytical solution for the accumulated pressure. Jeng and Seymour (2007) also developed an analytical solution for the same case, but in a form different from that given in Sumer and Fredsøe (2002). Jeng and Seymour showed, however, that their solution is actually identical to that of Sumer and Fredsøe (2002). Jeng and Seymour (2007) implemented their solution to determine the maximum liquefied depth. The latter authors comment that, although their solution is only valid for infinitely large soil depth, it provides a reasonable estimate for deep soil depths.

Finally, Dunn et al. (2006) adopted the code DIANA-SWANDYNE II (Dynamic Interaction and Nonlinear Analysis—Swansea Dynamic program version II) for waves, to study pore pressure variations (for both the phase resolved component and the period-averaged component). This code, developed for 2-D cases, uses the fully coupled Biot dynamic equation. The mathematical/numerical formulation of the code is described in detail by Chan (1988, 1995) and Zienkiewicz et al. (1990, 1999). The model includes a constitutive model that can predict both residual and momentary liquefaction. However, the constitutive model requires a large number of material parameters to describe the loading and unloading behaviour of the soil, usually obtained from detailed laboratory testing such as triaxial tests. Although the model has been validated for earthquake induced liquefaction, Dunn et al. (2006) implemented the model for wave loading; the model was tested against the analytical solution of Hsu and Jeng (1994); and the laboratory experiments of Teh et al. (2003). The latter experiments involve pore-pressure buildup, and liquefaction. The model, tested and validated, was subsequently implemented to study liquefaction around a buried pipeline.

2.3 Centrifuge modelling

Geotechnical centrifuge testing is a technique widely used in Geotechnical Engineering for physical modelling studies. There are two kinds of geotechnical centrifuges: (1) Arm centrifuges, and (2) Drum centrifuges. The former is, by far, the most popular one. The book edited by Taylor (1995) gives a detailed account of various aspects of geotechnical centrifuge technology. Schofield (1980) also can be consulted for basic principles behind centrifuge modelling, including some applications. The principal idea behind the centrifuge testing is as follows. In situ, stresses change with depth, and it is known that the soil behaviour (stress-strain relationship, friction angle) is a function of stress level. This implies that, in a regular physical model test, the soil behaviour will not be simulated correctly, because the stresses due to the soil self-weight are too low. In order to achieve the same stress level as in the prototype, in the case of the arm centrifuge, for example, soil specimen is placed at the end of the arm centrifuge, and the arm is rotated at a specified angular rotational speed so that the same stress level as in the prototype is achieved through the centrifuge acceleartion. The angular rotational speed can be determined by a simple analysis. The analysis shows that, in order to achieve the same stress level as in the prototype, the centrifugal acceleration should be selected as $a_m = Ng$ in which N is the model length scale, and g is the acceleration due to gravity.

Sassa and Sekiguchi (1999) implemented an arm centrifuge to study the sequence of liquefaction process under waves. The test setup is shown in Figure 2 with Figure 2a illustrating the setup prior to spinning and Figure 2b during spinning. The cross-section of the wave tank is indicated in the figures, the dark area in the cross section representing the sand pit. The length of the wave tank (from the wave paddle to the section with slotted partition to handle reflection) was 37 cm, and the sand pit was 20 cm in length and 10 cm in depth. Pore pressures at various locations were measured. Incidentally, Sassa and Sekiguchi reported the results of their subsequent work in a series of papers, among others, Sekiguchi et al. (2000), Miyamoto et al. (2003 and 2004). Earlier references for centrifuge wave testing include Sekiguchi and Phillips (1991), and Sekiguchi et al. (1995 and 1998).

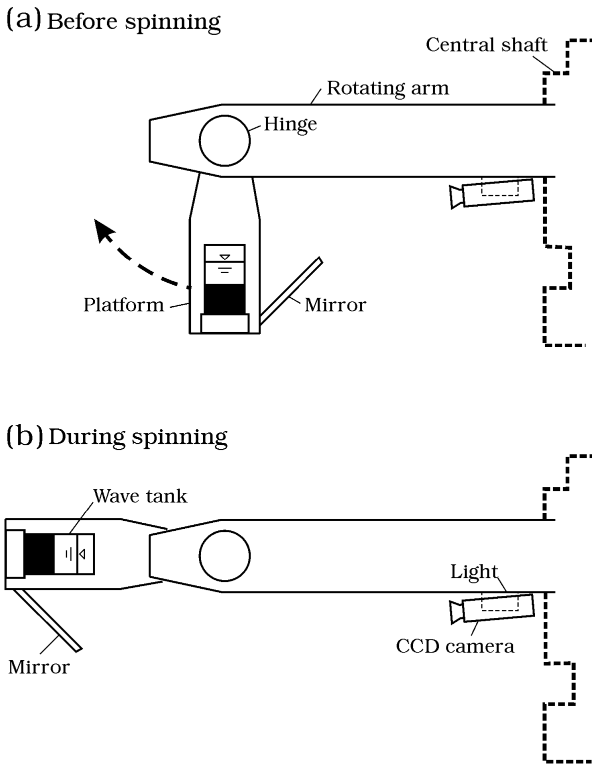

Figure 2 Arm centrifuge employed by Sassa and Sekiguchi (1999) for centrifuge wave testing.

Sassa and Sekiguchi (1999) showed that, in order to achieve a geometrical similarity between the model and the prototype wave, the model wave angular frequency should be selected according to

$$\omega_m = N\omega_p \tag{3}$$

in which ω_m and ω_p are the angular frequency of the model and prototype waves, respectively. They further showed that, for a model similarity regarding the buildup of pore pressure, the viscosity of the model liquid should be selected according to

$$\mu_m = N\mu_p \tag{4}$$

in which μ_m and μ_p are the viscosity of the model and prototype liquids, respectively. Furthermore, they also showed that, for a complete similarity of the pressure buildup, a third parameter, namely

$$\chi_0 = \left(\frac{\tau}{\sigma_{v0}'}\right)_{z=0} = \frac{p_b\lambda}{\gamma'} \tag{5}$$

needs to be kept in the model the same as in the prototype. Sassa and Sekiguchi (1999) named this parameter the wave severity. In the above equation, τ is the shear stress in the soil induced by the wave, σ_{v0}' is the initial vertical effective stress, p_b is the amplitude of the wave induced pressure on the bed, and λ is the wave number.

Eq. (4) implies that, for a model similarity, the model liquid should have a viscosity which is N times larger than the prototype liquid, normally sea water. This leads to a very viscous liquid. Sassa and Sekiguchi (1999) used silicone oil in their centrifuge experiments, corresponding to $N = 50$. Two kinds of tests were conducted in Sassa and Sekiguchi's (1999) study: Progressive-wave tests, and standing-wave tests. In the context of the present paper, we will consider the progressive-wave tests. The test conditions were as follows. Soil properties: Sand with $d_{50} = 0.15$ mm; the specific gravity of grains, $s = 2.65$; the maximum and minimum void ratios, respectively, $e_{max} = 1.07$ and $e_{min} = 0.64$; the relative density (or the density index), $D_r = 0.42$ (the relative density varied slightly over the tests carried out; D_r was 0.42 for two specific tests we will use in this paper); the void ratio, $e = 0.889$; the submerged specific weight of soil, $\gamma' = 428.5$ kN/m^3; and the soil depth, $d = 100$ mm. Wave properties: The water depth, $h = 90$ mm; the wave height, $H = 33.4$ mm (Test P5-1) (the wave height calculated from the small amplitude linear wave theory, corresponding to the measured pore pressure value at the mudline); the wave period, $T = 0.0909$ s; and the wave length, $L = 515$ mm (calculated from the small amplitude linear wave theory).

Considering the model scale, $N = 50$, and the fact that the sediment properties of the model experiments remain the same (as in the model), the model conditions of Sassa and Sekiguchi's (1999) centrifuge experiments correspond to the following field conditions (see Sumer, 2014, Chapter 3 for a detailed discussion): Soil properties: Sand with $d_{50} = 0.15$ mm; the specific gravity of grains, $s = 2.65$; the maximum and minimum void ratios, respectively, $e_{max} = 1.07$ and $e_{min} = 0.64$; the relative density, $D_r = 0.42$; the void ratio, $e = 0.889$; the submerged specific weight of soil, $\gamma' = 8.57$ kN/m^3 (calculated from $\gamma' = [(s-1)/(1+e)]\gamma$); and the soil depth, $d = 5$ m. Wave properties: The water depth, $h = 4.5$ m; the wave height, $H = 1.67$ m (Test P5-1); the wave period, $T = 4.5$ s; and the wave length, $L = 25.7$ m.

In principle, the results obtained by Sassa and Sekiguchi (1999) can be viewed as field data since the stress level in the centrifuge experiments was maintained precisely the same as in the field, and also the liquid in the model was selected such that a complete similarity between the model and prototype waves could be achieved. Therefore, in the following paragraphs, the Sassa and Sekiguchi (1999) results will be designated as field data (obtained through centrifuge experiments), and compared with similar results from standard wave-flume experiments of Sumer et al. (2006 a). It may be noted that this analysis has been carried out in Sumer (2014, Chapter 3), and the following subsection will present the highlights of this analysis.

2.4 Comparison with standard wave-flume results

From dimensional considerations, the period-averaged accumulated pore pressure, $\bar{p}$, can be described as a function of the following nondimensional quantities

$$\frac{\bar{p}}{p_{\max}} = f(\lambda z, \omega t, \chi_0, D_r, \lambda d, S) \qquad (6)$$

in which $p_{\max}$ is the maximum value attained by the period-averaged accumulated pore pressure for large times, λz is the nondimensional depth, ωt the nondimensional time, χ_0 is the wave severity parameter, Eq. (5), D_r is relative density of the soil, λd is the nondimensional soil depth, and S is a nondimensional parameter defined by

$$S = \frac{c_v T}{L^2} \qquad (7)$$

in which c_v is the coefficient of consolidation. The reader is referred to Sumer (2014, Section 3.3.3) for a detailed discussion of the latter nondimensional representation.

Sumer (2014) compared test data obtained from a standard wave-flume experiment (Sumer et al., 2006 a) with those from Sassa and Sekiguchi's (1999) centrifuge experiments. Two kinds of comparison were made, one with a pore pressure buildup with no liquefaction, and the second with liquefaction. Figure 3 displays the comparison where the pressure builds up with liquefaction. The test conditions in Sumer et al.'s (2006 a) standard wave flume experiment were as follows: Soil properties: Sand with $d_{50} = 0.060$ mm; the specific gravity of grains, $s = 2.65$; the maximum and minimum void ratios, respectively, $e_{\max} = 0.87$ and $e_{\min} = 0.46$; the relative density, $D_r = 0.38$; the void ratio, $e = 0.715$; the submerged specific weight of soil, $\gamma' = 9.44$ kN/m^3; and the soil depth, $d = 0.175$ m. Wave properties: The water depth, $h = 0.42$ m; the wave height, $H = 0.16$ m (Test 4); the wave period, $T = 1.6$ s; and the wave length, $L = 2.9$ m. Figure 3 essentially compares the time series of the period-averaged pressure from the "field" test obtained through Sassa and Sekiguchi's (1999) centrifuge experiment with that obtained from Sumer et al.'s (2006a) standard wave-flume experiment. Comparison is made on the basis of the nondimensional representation in Eq. (6). The values and/or ranges of the governing parameters in the latter equation are indicated in the inset of Figure 3. Note that the pore pressure measurement of Sassa and Sekiguchi was made at the depth $z = 0.5$ m in the field (or $z = 10$ mm in the centrifuge), whereas that of Sumer et al. at the depth $z = 5.5$ cm in the standard wave flume test. Nevertheless, notice that the nondimensional z values, namely λz values, of the two experiments are identical.

Although there are differences in the values of the nondimensional parameters χ_0 and D_r, and more significantly in the values of λd and S, the agreement between the standard wave-flume experiments and the centrifuge "field" experiments exhibited in Figure 3 is striking. A similar agreement was obtained in the other comparison exercise mentioned earlier where the pore pressure builds up, but liquefaction does not occur (see Sumer 2014, Figs. 3.36 and 3.37). This has the following implication: Standard wave-flume tests can also be used for physical modelling study of buildup of pore pressure and liquefaction provided that the results should be analyzed and interpreted on the basis of the nondimensional representation described in Eq. (6). Now, recall the soil depth in the above "field" experiment, namely d = 5 m. In the corresponding centrifuge tests, the stress level associated with this depth was truly replicated, and therefore the soil behaviour (stress-strain relationship, friction angle) was reproduced as in the field. Since the buildup of pore pressure (both in the no-liquefaction regime and in the liquefaction regime) appear to be in very good agreement with that obtained in the standard wave-flume experiments, it can be inferred that the change in the soil behaviour with depth is apparently not significant for such "shallow" soil depths. Since the wave-induced buildup of pore pressure and liquefaction is, for the most part, associated with shallow soil depths, the classic standard wave-flume tests appear to be a viable option for physical modelling studies of wave-induced liquefaction.

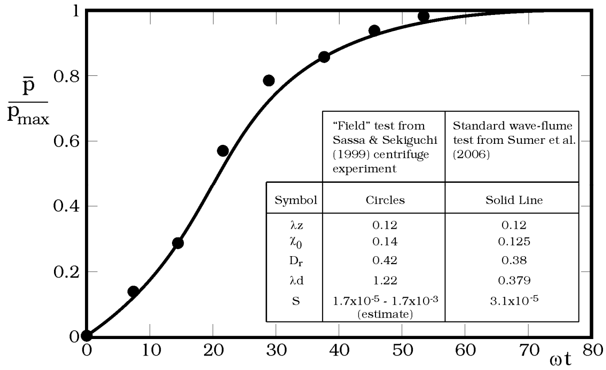

Symbol	"Field" test from Sassa & Sekiguchi (1999) centrifuge experiment	Standard wave-flume test from Sumer et al. (2006)
	Circles	Solid Line
λz	0.12	0.12
χ_0	0.14	0.125
D_r	0.42	0.38
λd	1.22	0.379
S	$1.7\text{x}10^{-5}$ - $1.7\text{x}10^{-3}$ (estimate)	$3.1\text{x}10^{-5}$

Figure 3 Comparison between Sassa and Sekiguchi's (1999) 50g centrifuge results and Sumer et al.'s (2006 a) 1g standard wave-flume results.

2.5 Other issues

2.5.1 Mathematical modelling of compaction

As described in Section 2.1, the liquefaction is followed by the compaction where the upward-directed pressure gradient (generated by the liquefaction) drives the water in the liquefied soil upwards while the soil grains "settle", leading to a progressive compaction of the liquefied soil, starting from the impermeable base. Sumer (2014, Section 3.4) developed a simple mathematical model for the compaction process. The model predicts the velocity of the compaction front as

$$U_c = \frac{c}{1-n_1}(1-c)^{2.7} w_0 \qquad (8)$$

in which c is the volume concentration corresponding to the liquefied soil, which can be calculated from Sumer et al.'s (2006 b) mathematical model developed for the density of liquefied soil. The quantity n_1 in Eq. (8) is the porosity of the compacted soil, and w_0 is the fall velocity of sediment grains in dilute concentration. The above equation, Eq. (8), enables one to predict the time scale of the compaction process, namely the time period from the instant where the compaction starts at the impermeable base to the that where the compaction front reaches the mudline. Sumer (2014, Section 3.4) tested and validated the model against laboratory data. A numerical example covering a field situation is also given in the latter reference.

2.5.2 Influence of clay content

The seabed in the previous sections is considered to contain one type of soil such as silt. However, it is not uncommon that the seabed may contain clay, and therefore the seabed soil in these cases acts as a composite soil such as, for example, clayey silt or clayey sand. Kirca et al. (2014) conducted liquefaction experiments to study the influence of clay content in such soils. It turns out that the influence of clay content is very significant. The experiments in Kirca et al.'s study were, for the most part, made with silt and silt-clay mixtures, which were complemented with some tests made with sand-clay mixtures. It was found that susceptibility of silt to liquefaction is increased with increasing clay content, CC, up to $CC \approx 30\%$ (which is clay specific), beyond which the mixture of silt and clay is not liquefied. It was also found that sand may become prone to liquefaction with the introduction of clay, contrary to the general perception that sand is liquefaction resistant under waves. For instance, sand with $d_{50} = 0.4$ mm was liquefied with a clay content of $CC = 10.8\%$, while sand with $d_{50} = 0.17$ mm was partially liquefied with CC as small as $CC = 2.9\%$.

This kind of behavior is described in Kirca et al. (2014) in terms of the micro-fabric of the mixtures. (The latter was studied by Gratchev et al., 2006, by means of scanning electronic microscope.) For example, silt-clay mixture was not liquefied for the values of clay content greater than $CC \approx 30\%$ because the silt grains are encapsulated completely with clay matrixes, and therefore the silt grains cannot rearrange under cyclic shear strains due to the cohesive character of the mixture, presumably leading to resistance to liquefaction. Kirca et al. (2014) linked the increased susceptibility of silt to liquefaction with increasing clay content, CC (up to $CC \approx 30\%$) to the permeability of the silt and clay mixture. The larger the clay content, the smaller the permeability, and therefore the silt-clay mixture should have a larger susceptibility to liquefaction with increasing clay content.

2.5.3 Influence of cover stones

Surface protection by cover stones over a liquefiable soil (e.g., backfill soil, silt or fine sand, in a trench) is a method to protect the soil against scouring. Scouring may be caused by effects such as current, combined wave and current, and wave-induced steady streaming near the bed. A fairly substantial amount of knowledge has been gained on the behavior of cover stones/riprap on a liquefaction-resistant sediment bed in the past decade or so (see e.g. Sumer and Fredsøe, 2002). However, relatively little study has been done on the behaviour of cover stones/riprap on a liquefiable sediment bed, Sekiguchi et al. (2000) and Sumer et al. (2010). The questions are (1) Can a liquefaction-prone soil underneath such a protection system be liquefied even if it is fully covered? (2) Can cover stones be used as a counter measure against liquefaction? (3) What is the effect of a filter layer used between the cover stones and the soil? (4) What is the behavior of the cover stones if the soil underneath is liquefied (issues involving sinking of the stones and their penetration distance)?

Sumer et al.'s (2010) study (substantiated by the Sekiguchi et al., 2000, work) demonstrated that a liquefaction-prone soil can be liquefied under a stone protection cover if the accumulated pore-water pressure exceeds the value of the initial mean normal effective stress, calculated by

$$\sigma_0' = (\gamma' z + p_s)\frac{1+2k_0}{3} \tag{9}$$

in which p_s is the surface loading (or the surcharge) corresponding to the cover stones. In the case of not-too-shallow soils, the quantity p_s in the above equation is to be replaced by αp_s in which α is a factor related to the spreading of the loaded area with the soil depth, and can be taken from the chart where contours of increase in vertical stress below a strip footing are plotted as function of depth and horizontal extent, e.g., Powrie (2004, p. 337). "Not-too-shallow-soils" can be defined as those soils with soil depths larger than $O(0.5B)$ in which B is the width of the strip footing.

As the above equation implies, cover stones is a viable option as a counter measure against liquefaction. This is simply because the accumulated pore pressure will not be able to reach the value of the initial mean normal effective stress if the surcharge, p_s, is sufficiently large. Sumer (2014, Chapter 11) discusses in greater details this option among others including the effect of filter layers as counter measures against liquefaction.

Although it is only of academic interest, it is interesting to note the following observation made in Sumer et al. (2010): The latter authors also did experiments with very densely packed stone covers. In these latter experiments the stones were arranged like a "jigsaw puzzle". In these tests, even with one-layer stone cover, the soil underneath was not liquefied. It is important to note that this was for the same wave conditions under which the soil was liquefied with even two-layer stone cover. Sumer et al. (2010) linked this to the diminished expansion and contraction of the soil under such densely packed stone cover.

Regarding the question about the behavior of the cover stones when the soil underneath is liquefied (which may involve issues like sinking of the stones and their penetration distance), this will be discussed in Section 5.1 below.

2.5.4 Residual liquefaction in combined waves and current

It is known that when a wave encounters a current, the wave characteristics change, with the wave height and the wave length changing as function of the current velocity, meaning that the bed pressure will also change with the current velocity. Clearly, in this case, a new wave loading will be generated, and therefore the soil will undergo cyclic shear stresses/strains induced by this new wave loading. Sumer (2014, Section 3.7) studied in a systematic manner the influence of the current on liquefaction potential under a given set of wave and current conditions.

The principle idea of handling the combined waves and current situations is to calculate the new wave height, the new wave length and the new water depth with the introduction of the current for a given set of wave parameters. (With the introduction of the current, the wave period will not change.) Sumer (2014, Section 3.7) present charts for the aforementioned new wave height, wave length and water depth as a function of two nondimensional parameters, namely Ω_0 and Fr_0:

$$\Omega_0 = \omega\sqrt{\frac{h_0}{g}}, \tag{10}$$

$$Fr_0 = \frac{U}{\sqrt{gh_0}} \tag{11}$$

in which h_0 is the water depth in the "undisturbed" case (i.e., before the current is introduced), and U is the current velocity. The analysis shows that the opposing current causes the wave height to increase and the wave length to decrease (with not too significant change in the water depth). The latter effects will clearly increase the susceptibility of soil to liquefaction. A numerical example given in Sumer (2014, Section 3.7) illustrates this conclusion quite clearly.

3. MOMENTARY LIQUEFACTION

3.1 Assessment of momentary liquefaction

As mentioned in Section 1, momentary liquefaction occurs during the passage of the wave trough. Under the wave trough, the pore-water pressure (in excess of the hydrostatic pore-water pressure) has a negative sign. If the soil is unsaturated (the soil containing some air/gas), the pore-water pressure will be "dissipated" very fast with the depth. A pore pressure distribution (with pressures being negative, and strongly dissipating with the depth) will generate a substantial amount of lift at the top layer of the soil under the wave trough. If this lift exceeds the submerged weight of the soil, the soil will fail, i.e., it will be briefly liquefied. The upward-directed large pressure gradient, the lift force, is caused by the air/gas content of the soil. It may be mentioned that only a very small amount of gas (less than 1%) would be enough to cause a very large dissipation of pore pressure with the depth, and therefore a very large lift force. We shall return to the air/gas content issue later. It may be noted that in order for the soil to be liquefied due to momentary liquefaction, the soil will have to be unsaturated, illustrated by an analysis carried out by Sumer (2014, Section 4.2). The latter analysis is based on the solution of the Biot equations developed by Yamamoto et al. (1978) for saturated soils and for infinitely large soil depths.

Sumer (2014, Section 4.3) also present an analysis to cope with the unsaturated soil case, with both infinitely large soil depths, and finite soil depths. The analysis is based on (1) Mei and Foda's (1981) solution for the pore-water pressure for the case of the infinitely large soil depth, similar to the analysis carried out first by Sakai et al. (1992), and (2) Hsu and Jeng's (1994) solution for the case of the finite soil depth. These two cases were furnished with two numerical examples, to illustrate issues like whether or not momentary liquefaction occurs for a given set of soil and wave parameters; and the liquefaction depth in the case when the momentary liquefaction occurs.

Sumer (2014, Chapter 4) also addresses issues like momentary liquefaction and densification (Zen and Yamazaki, 1990 a and b), and momentary liquefaction in solitary waves over a horizontal sea bottom and on coastal slopes.

3.2 Air/gas content in marine soils

Air/gas content in marine soils is essential for momentary liquefaction, as discussed in the preceding paragraphs. There are direct and indirect evidence of presence of air/gas bubbles in the coastal and offshore environment, e.g., in tidal areas in coastal regions where the seabed is exposed to air and water alternately.

Mory et al. (2007) measured pore water pressure distribution across the soil depth on a tidal beach (the measurement depth being across the top 1 m layer), located in Capbreton, France. They, in a follow-up publication (Michallet et al., 2009), reported further analysis of the data collected in Mory et al. (2007). Mory et al. in their 2007 study found that momentary liquefaction occurred over significant portions of time, suggesting that the soil was unsaturated. This prompted Mory et al. (2007) (see also Michallet et al., 2009) to conduct a geoendoscopic video recording of the soil near the bed surface to observe visually whether or not the soil contained air bubbles. To this end, images of a 25 mm^2 area with a magnification of 10 were acquired. This study showed the presence of significant quantities of air inside the soil, down to 0.50 m, and vanishing with the depth beyond this level. Figure 4 illustrates a recorded image of air bubbles with an accompanying picture showing the processed image where the bubble images were singled out. As seen, the bubble size is in the same order of magnitude as the grain size, d_{50} being $d_{50} = 0.35$ mm. Figure 5 is reproduced from Michallet et al. (2009), illustrating the gas content versus the depth. Mory et al. (2007) link the presence of air bubbles to the tidal variations: Air is introduced inside the soil at low tide when the water level is below the soil level. When the water level rises with the high tide, the soil saturation will not be fully completed; some air bubbles will be trapped inside the soil, and remain there until the next tide cycle. Mory et al. (2007) explains, on the other hand, the very small air content within the top 0.10 m soil layer in terms of the mobility of the surface sediment at this top layer; the fact that the soil is constantly being reworked by sediment transport will help air bubbles escape the bed.

An indirect piece of evidence of potential presence of air comes from Tørum's (2007) analysis of a set of field data obtained from extensive measurements of pore water pressure carried out by de Rouck (1991), de Rouck and van Damme (1996), and de Rouck and Troch (2002). These measurements were carried out in connection with the planning of the extension of the Zeebrugge Harbour, Belgium. They were conducted in two kinds of soils, sand and clay. Tørum (2007) compared the measured pressure distributions with those calculated from Mei and Foda's (1981) solution (see also Sakai et al., 1992 a), referred to above.

Hattori et al. (1992) and Sakai et al. (1992 b) also fitted Mei and Foda's (1981) solution to field data, "tuning" the apparent bulk modulus of elasticity of water so that they could obtain a reasonable match between the data and the Mei and Foda (1981) solution. Their results suggest the presence of air in seabed soil, similar to Tørum (2007).

Sills et al. (1991) stated that gas bubbles may form in the offshore environment where the methane is generated around nuclei of bacteria locally within a soft, consolidating soil. They report that the gas bubbles produced in this way are considerably larger than the fine grained soil particles, and the resulting soil structure consists of large bubble "cavities" within a matrix of saturated soil. (Incidentally, the latter authors developed a laboratory technique to mimic as closely as possible the process of bubble formation in the offshore environment.)

Various attempts have been made in the past to develop samplers for measurement of gas content in soils. These efforts have indicated that this is not a straightforward task. A review of the existing work has been given in Sandven at al. (2004). Recently, a new sampler that enables in-situ measurement of gas content in the seabed has been developed under the EU research program "Liquefaction Around Marine Structures (LIMAS) (2001-2004)" by Sandven et al. (2007). The latter authors pointed out that previously developed samplers for gassy soils utilize sealing methods such as inflatable membranes, ball valves for sealing pressurized core barrels, and plate valves or core catchers for the same purpose, while the aim of their study, they stressed, was to develop a sampler enabling measurement of the gas content, and at the same time retrieving a representative soil sample, making it possible to determine both the relative gas content and the degree of saturation in the soil. The developed sampler was used successfully at the LIMAS research site in Capbreton, France, the site Mory et al. (2007) (also reported in Michallet et al.'s, 2009) did their measurements; see the preceding paragraphs.

Figure 4 Image of air bubbles from geoendoscopic video recording of the soil near the bed surface on a tidal beach with an accompanying picture showing the processed image where the bubble images were singled out, Mory et al. (2007). Digital image: By courtesy of Professor Mathieu Mory of Univ. of Pau.

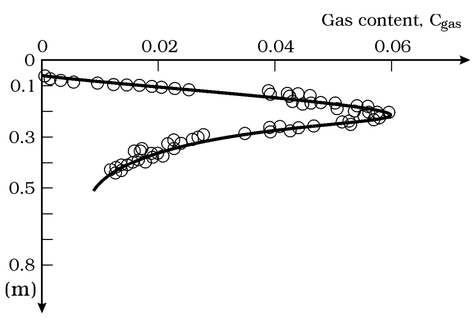

Figure 5 Gas content versus depth, measured in Michallet et al. (2009). The gas content was calculated from the image analysis of the geoendescopic video camera recording.

4. FLOATATION OF PIPELINES

4.1 Problem statement

The stability of pipelines buried in loose granular soils is of major concern in practice. Of particular interest is the potential for floatation of gas pipelines. The specific gravity of a gas pipeline can be as low as 1.6. When buried in a soil which is vulnerable to liquefaction, the pipeline can float to the surface of the soil simply because its density is smaller than that of the liquefied soil. Similar floatation problems may also arise for sea outfalls. Therefore it is important to determine the "critical" pipeline density below which the pipeline floatation occurs. It is also equally important to determine the density of liquefied soil so that assessments could be made whether or not there is potential for pipeline floatation for a given set of soil, wave and pipeline parameters. There are many reported incidents in the literature (see, e.g., Sumer, 2014, Chapter 5). Apart from the reported incidents, there are also pipeline failures for which information never entered into the public domain. The field observations and laboratory experiments suggest that liquefaction of soil for trenched/buried pipelines must be a design condition to check for pipeline stability for floatation. This is particularly important for light pipelines.

An extensive review of the subject was given in Sumer (2014, Chapter 5), which indicated that the work done until mid-2000s presented a highly confusing picture; there was a great deal of uncertainty on the values of the critical pipe density for floatation, and on the density of liquefied soil. The questions appeared to be: (1) What is the critical floatation density of pipelines buried in a soil where the soil is undergoing wave-induced liquefaction? (2) Is the latter a constant set of value? Does it vary across the soil depth? (3) What is the density of liquefied soil? (4) What are the parameters which govern the density of liquefied soil? These questions have been addressed in a relatively recent study by Sumer et al. (2006 b). The following paragraphs will mainly give the highlights of this latter study.

4.2 Density of liquefied soil

In order to determine the density of liquefied soil, Sumer et al. (2006 b) did experiments with model pipes. The model pipes (heavier or lighter than the liquefied soil) were buried in the soil. The lighter pipes floated towards the surface of the bed while the heavier pipes sank in the soil, with the liquefaction of the soil by waves (residual liquefaction). The pipes have, in the tests, acted as a hydrometer, the instrument to measure density of liquids. The pipe remained where it was when its density was equal to the density of the surrounding liquefied soil; or it stopped in its upward or downward motions at the point where its density was equal to that of the surrounding liquefied soil. Having known the density of the pipe, the density of the liquefied soil could be determined from these experiments. The data indicated a slight increase of the density of the liquefied soil with the depth,

$$s_{liq} = 0.18\frac{z}{d} + 1.85 \qquad (12)$$

the quantity d being the soil depth. Sumer (2014) compared the above result with those from Teh et al. (2006) and found a remarkable agreement. The above equation indicates that the density of the liquefied soil is 1.85 at the surface of the bed while it increases to a value of 2.03 at the impermeable base.

Sumer et al. (2006 b) have also developed a mathematical model for density of liquefied soil. The model is based on the force balance equation (in the vertical direction) for a soil grain settling in the liquefied soil. The latter involves the kinematic viscosity of water, and fall velocity of grains as being functions of solid concentration, c . The model equation eventually reduces to an equation which is to be solved for the concentration, and, from the latter information, the density of the liquefied soil is obtained from

$$s_{liq} = (1-c) + c\frac{\gamma_s}{\gamma} \qquad (13)$$

in which s_{liq} is the specific gravity of the liquefied soil. Sumer et al. (2006 b) tested and validated their model against Teh et al.'s (2003) experiments.

The mathematical model tested and validated has been implemented to study the influence of the three governing parameters, γ_s/γ , γ_t/γ and k_0 , on the specific gravity of liquefied soil. Here, γ_s and γ_t are the specific weight of soil grains and specific weight of soil, respectively, and k_0 is the coefficient of lateral earth pressure.

The time of travel of a floating pipe may also be a concern in practice. In order to make an estimate of this quantity, Sumer (2014, Chapter 5) used the following approach.

Sumer et al.'s (1999) laboratory tests of pipe displacements (floatation or sinking) indicate that the pipe motion reaches a steady state (in which the pipe moves with a practically constant velocity) shortly after the onset of the motion. Clearly the motion will not be steady near the initiation and termination of the motion. Nevertheless, it may be assumed that, for the most part, the pipe moves in a steady state. In this steady-state pipe motion, the forces acting on the pipe in the vertical direction should be in balance, these forces being the buoyancy force and the drag force. The aforementioned force-balance equation, when solved for the floatation velocity in the case of a floating pipe, gives:

$$w = \left(\frac{\pi D g}{2C_D}\frac{s_{liq}-s_p}{s_{liq}}\right)^{1/2} \qquad (14)$$

in which w is the floatation velocity, D is the pipe diameter, s_p is the pipe specific gravity, and C_D is the drag coefficient corresponding to the pipe motion in a liquefied soil, and given in Sumer (2014, Chapter 6). The time scale of the pipe's floatation motion may be determined from $T_{float} = L_{float}/w$ in which L_{float} is the vertical distance travelled by the floating pipe.

Sumer (2014, Chapter 5) also discusses a stability design approach described in Damgaard et al. (2006), and floatation due to momentary liquefaction (Maeno et al., 1999).

5. SINKING OF PIPELINES AND MARINE OBJECTS

5.1 Process of sinking

As mentioned previously, pipelines laid on the seabed may sink (self-burial of pipelines), large individual blocks (like those used for scour protection) may penetrate into the seabed, sea mines may enter into the seabed and eventually disappear, caisson structures may burrow into the seabed. Floatation of pipelines in a liquefied soil has been discussed in the previous section. This section focuses on sinking of pipelines, and marine objects such as individual blocks (stones, etc.) in a liquefied seabed. Incidents of this nature have been quoted in the literature. Yet, there have been many unreported cases where structures have suffered considerable damages as a consequence of liquefaction failure of the soil and the resulting sinking. It may be noted that sinking of pipelines is a concern in practice, as large longitudinal forces can be induced by the pipe deflection (Brown, 1975, Herbich, 1981). (Herbich, 1981, notes, however, that these stresses are unimportant unless they are generated near the pipe riser.)

Sumer et al. (1999) investigated the sinking/floatation of pipelines and marine objects (cube- and spherical-shaped) in a liquefied soil. In a later study, Sumer et al. (2010) studied sinking of cover stones. In both studies, the liquefaction was due to the buildup of pore pressure. Similar experiments were carried out by Teh et al. (2003 and 2006).

Sumer et al.'s experiments with circular pipes, sphere- and cube-shaped objects (Sumer et al., 1999), and with stone covers (Sumer et al., 2010), Teh et al.'s (2003 and 2006) experiments with circular pipes, and Kirca's (2013) experiments with irregular-shape blocks, all showed that the objects (buried or lying on the bed) begin to sink in the soil when liquefaction sets in with the introduction of waves. Provided that the density of the object is not in the narrow range of the liquefied-soil density, but rather larger than the upper bound of that range, namely, $s_p > 2.03$ (i.e., provided that the object does not act as a hydrometer), the above mentioned work indicate that the downward motion of the object terminates before it reaches the impermeable base. Sumer et al.'s (2010) work showed that the mechanism of the termination of the downward motion is as follows, Figure 6: (1) The object begins to sink in the liquefied soil (Panel 1); (2) The object's downward motion terminates when it meets the compaction front, which is travelling upwards (Panel 2); and (3) The object is fully stopped ("arrested" in the compacted soil), as the compaction front continues to move upwards (Panel 3).

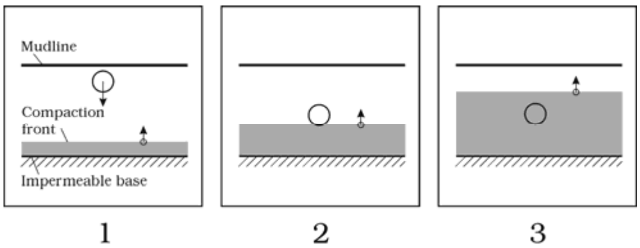

Figure 6 Process of sinking of an object in liquefied soil. Object's sinking terminates when it meets the compaction front.

5.2 Drag coefficient

Various features of the sinking of pipelines and other objects have been described in Sumer et al. (1999), Teh et al. (2003, 2006) and Kirca (2013). Of these, drag on a sinking object should be specifically noted. Sumer et al. (1999) calculated the drag coefficient, using the fall velocity data they obtained in their experiments. However, in their calculation, they assumed that the specific gravity of liquefied soil, s_{liq}, was 1.3, an incorrect value. This was due to the lack of knowledge/data on this quantity at the time of their study. In Sumer (2014, Chapter 6), Sumer et al.'s (1999) data have been recast with s_{liq} taken as 1.94 (a depth-averaged value; see Eq. (12), Section 5.3), and plotted against the pipe Reynolds number. This exercise showed that the drag coefficient decreases with increasing Reynolds number, and appears to attain an asymptotic value of $O(10^7)$, a value which is a multiple orders of magnitude larger than the ordinary fluid drag (Schlichting, 1979, p. 17). Sumer (2014, Chapter 6) also discusses the drag coefficient for sphere- and cube-shaped bodies, and Kirca (2013) for irregular shape blocks.

The above discussion concerns the situations where liquefaction is due to buildup of pore pressure (residual liquefaction). For momentary liquefaction scenarios, no study is yet available, investigating the sinking/floatation of pipelines under momentary-liquefaction regime. This may be due to the fact that it is difficult to produce the momentary liquefaction in a small-size wave flume using a normal sand bed, as pointed out by Sakai et al. (1992). However, Chowdury et al. (2006) studied the sinking of short pipes, using a cylindrical column to get around the problem associated with small-scale wave flume facilities. Sakai et al. (1994) report an extensive series of laboratory experiments where the block subsidence due partly to the momentary liquefaction and partly to the oscillatory flow action has been investigated. Maeno and Nago (1988) present the results of an experimental study where the effect of a progressive wave is simulated by an oscillating water table. A concrete, rectangular-prism-shaped block sitting initially on the surface of the soil gradually sank, as the oscillating movement of the water table continued. A similar approach was also adopted by Zen and Yamazaki (1990 a) to observe sinking of a rectangular-prism-shaped heavy object under momentary-liquefaction conditions. Similar to pipelines, although the problem of sinking/subsidence of armour blocks, sea mines etc. in soils subject to momentary liquefaction has been recognized widely, no study is yet available investigating this problem in a systematic manner.

6. LIQUEFACTION AT GRAVITY STRUCTURES

6.1 General description

Gravity structures are used invariably in Marine Civil Engineering, e.g., caisson breakwaters (or vertical-wall breakwaters), gravity-base offshore platforms, gravity-base foundations of offshore wind turbines, gravity-base caissons (or box caissons), used as "building blocks" of berths at port terminals, or bridge piers, etc.

Buildup of pore-water pressure around and under such structures may strongly affect the processes associated with the failure of foundations of these structures. Both the slip-surface failure and the excess settlement failure, two of the most important failure modes (Coastal Engineering Manual, 2006, Chapter 2, Part 6), may be affected by the accumulation of pore-water pressure. If the buildup of pore-water pressure eventually leads to liquefaction, this will obviously lead to direct failure of the structure.

The subject can possibly be best described with reference to a breakwater, a gravity structure. Consider a progressive wave (the incident wave) approaching the breakwater, Figure 7. As this wave impinges on the offshore face of the breakwater, a reflected wave will be created moving in the offshore direction, and, as a result, these two waves will form a standing wave in front of the breakwater. There are two zones with liquefaction potential, Zone 1 and Zone 2. In the former (Zone 1), pore-water pressure can build up under the standing wave, which may lead to liquefaction if the wave height is large enough and sediment is fine and in the loose state. In the latter (Zone 2), the pore-water pressure may also build up under the structure. This is generated by two different mechanisms, namely (1) by wave motion, and (2) by caisson motion. In the former, wave-induced pressure will be transferred onto the seabed through the rubble-mound bedding layer. In the latter, the waves will generate cyclic overturning moments, resulting in a rocking motion of the structure, which will be transferred to the seabed in the form of cyclic bed pressure underneath the breakwater.

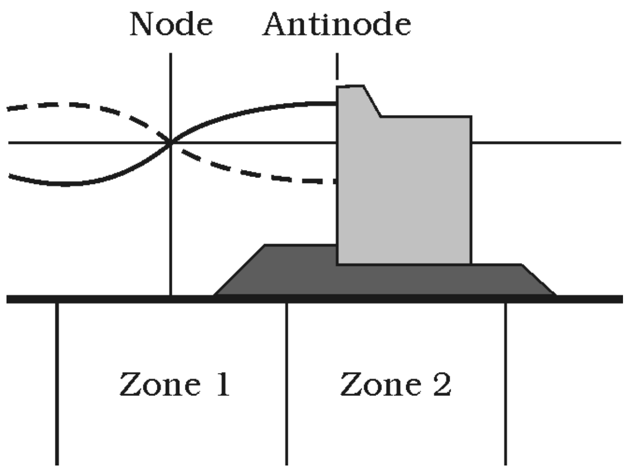

Figure 7 Potential liquefaction zones. Schematic.

6.2 Liquefaction beneath standing waves

Sekiguchi et al. (1995) and Sassa and Sekiguchi (1999) used centrifuge wave testing to study liquefaction in standing waves. The test setup in Sassa and Sekiguchi's (1999) study was designed such that the antinode of the standing wave formed in the middle of their sediment pit. Their pore pressure measurements indicated that liquefaction occurred at the antinodal section, although soil experiences no shear strains at this section.

Kirca et al. (2013) studied liquefaction beneath standing waves in a standard wave flume. The experiments show that the seabed liquefaction beneath standing waves, although qualitatively similar, show features different from that caused by progressive waves. The pore water pressure builds up in the areas around the node and subsequently spreads out toward the antinodes. The experimental results imply that this transport is caused by a diffusion mechanism with a diffusion coefficient equal to the coefficient of consolidation. The experiments further show that the number of waves to cause liquefaction at the nodal section appears to be equal to that experienced in progressive waves for the same wave height.

Sassa and Sekiguchi (2001) used a cyclic-plasticity constitutive model to account for the effect of stress axis rotation of sand. The model was then applied to soil responses to progressive and standing-wave loadings. Using the model, Sassa and Sekiguchi (2001) simulated their centrifuge wave tests from Sassa and Sekiguchi (1999). In addition to the latter, Sassa and Sekiguchi (2001), in their numerical study, carried out an idealized test where they extended the sediment pit such that the entire length of the sediment pit covered nearly one full wave length, with three antinodes (one in the middle of the sediment pit and the other two at the onshore and offshore ends of the pit), and two nodes between the three antinodes. This enabled them to observe what happens at the nodal and anti-nodal sections in their numerical simulation, with (nearly) free of end effects. This test showed that, although liquefaction conditions are not reached in the test, the accumulated pore pressure is markedly larger at the nodal sections than at the antinodal sections, consistent with the description given in the previous paragraph. It is interesting to quote Sassa and Sekiguchi (2001): ".. the liquefied zone develops first at the node and then extends laterally and vertically to neighbouring points. Thus soil behaviour at the antinode might be influenced by the liquefaction that (takes) place at points near the node, eventually undergoing liquefaction as well."

6.3 Liquefaction under the structure

Kudella et al. (2006), in a large-scale wave flume experiment (the flume length being 307 m, the width 5 m, and the depth 7 m) carried out tests with a model caisson breakwater placed on sand simulating the subsoil with a thin clay layer on the surface (Kudella et al., 2006, Figure 9). One of the findings of Kudella et al. (2006) was that the accumulated (residual) pore pressures generated in the subsoil under the breakwater were due to caisson motions alone (the rocking motion), the wave contribution being negligible. It may be noted that similar results were also obtained by Rahman et al. (1977, p. 1428) for a gravity-base offshore oil tank. This result is important in the sense that the processes related to the pore pressure buildup can be studied in the laboratory with a test setup where the model breakwater executes a rocking motion induced by an "overturning" moment, in the absence of waves. (Incidentally, in Kudella et al.'s, 2006, experiments, the rocking motion, large enough to generate pressure buildup, could only be induced by severe breaking wave impacts. Non-breaking waves did not generate pressure buildup.)

The above finding prompted Sumer et al. (2008) to employ a simple breakwater-foundation model, to study the buildup of pore pressure in the subsoil. This enabled Sumer et al. (2008) to make a detailed study of the buildup of pore pressure in the subsoil in a simple, idealized environment. The idea in Sumer et al.'s (2008) study was not to simulate what occurs in the field under the complex, combined action of waves and the rocking motion of the breakwater, but rather to single out the process of buildup of pore pressure due to the cyclic overturning moment (and therefore rocking motion) alone. Foundation of the caisson was simulated by a rectangular plate, slightly buried in the soil. Pore-water pressures were measured. With the rocking motion of the caisson, the pore-water pressure first builds up, reaches a maximum value and begins to fall off, and is eventually dissipated, the same kind of behavior in undisturbed cases, such as in progressive waves and in standing waves. The effect of amplitude and period of the caisson motion on pressure buildup was investigated in detail. The influence of the size and shape of the caisson were also investigated in Sumer et al. (2008).

Sumer (2014, Chapter 8) presents an extensive review of the literature. The review particularly addresses the question "Does pressure buildup under a typical gravity structure reach liquefaction levels?" (see also de Groot et al., 2006). Sumer (2014, Chapter 8) also includes a section describing how to make assessment of residual liquefaction potential for gravity-base structures, with a numerical example in which a caisson structure sitting on a silty sand bed, and exposed to normally incident waves is considered. Sumer (2014, Chapter 8) further discusses the overall effect of liquefaction, and also the generally observed seaward tilting of such structures.

The previous paragraphs highlight recent advances in residual liquefaction at gravity-base structures. A great many works have been devoted to the investigation of the phase-resolved pore-water pressure (with no residual component) and soil stresses around a breakwater, including the associated momentary liquefaction. (Recent work has been reviewed in the paper by Jeng et al., 2012.) Jeng et al. (2013) developed a numerical solution, and presented the method describing the way in which the momentary liquefaction is handled for a composite breakwater. They used an integrated model which combines (1) Volume-averaged Reynolds-averaged Navier Stokes (VARANS) equations for the wave motion in the water as well as in the porous structure (the rubble mound in the present case), and (2) the dynamic Biot equations for the seabed. A one-way coupling method was developed to integrate the VARANS equations with the dynamic Biot equations. The dynamic Biot equations are essentially an extension of the Biot equations (Chapter 2) where the accelerations of the pore water and soil particles are considered while the displacement of pore water relative to soil particles is ignored. The authors verified their model against a set of experimental data from various sources.

Finally Michallet et al. (2012 a) report momentary liquefaction observed in a laboratory experiment where a single wave consisting of a trough and followed by a crest breaks on a vertical wall placed on a 1:20 slope. Michallet et al. (2012 a) measured the free-surface elevation at the wall and pore-water pressures just below, at four depths, and demonstrated that upward-directed pressure-gradient forces were generated near the surface of the sediment bed, which have large enough for the sediment to undergo momentary liquefaction. They used in the experiments 0.64 mm grain size light-weight material with a density of 1.18. The bed was initially unsaturated with an estimated amount of air content of 4%. The authors observed strong motions in the bed down to 15 cm depth. These motions were recorded, using Particle Image Velocimetry (PIV). In addition to particle velocity, the strain tensor modulus, the vorticity and the divergence were obtained. In a parallel study, Michallet et al. (2012 b) carried out tests under periodic waves, with the results similar to the case of the single wave, Michallet et al. (2012 a).

7. STABILITY OF ROCK BERMS IN LIQUEFIED SOILS

There are basically three kinds of protection measures for pipelines: (1) the pipeline may be laid in a trench; (2) it may be covered with a stone protection layer; or (3) it may be covered with a protective mattress (see, e.g., Sumer and Fredsøe, 2002). This section is concerned with the first kind of protection.

A viable option for this kind of protection is to install a rock berm over the pipeline. There are two scenarios related to this option. The trench and the rock berm are left open (Figure 8 a). However, in this case, the trench may be backfilled due to sediment transport, the natural backfilling (Figure 8 b); or, following the installation of the rock berm, the trench is backfilled intentionally with the in-situ sediment (Figure 8 b). The sediment in both cases (being in the loose state because the backfilling processes involve slow sedimentation) may be susceptible to liquefaction under waves. With the liquefaction of the sediment, internal waves emerge at the interface between the liquefied sediment and the water column, and consequently the liquefied sediment experiences an orbital motion. With this, the rock berm will be exposed to the motion of liquefied soil.

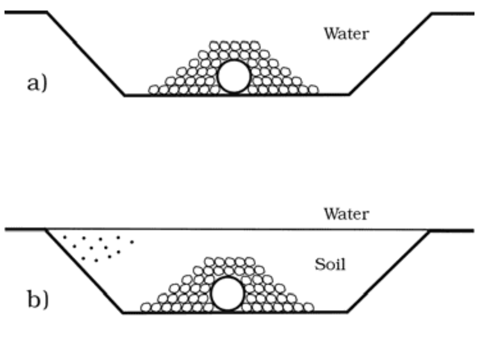

Figure 8 (a) Installation of a rock berm over a pipeline. (b) The trench is backfilled (naturally or intentionally).

The conventional design strategy for a rock berm exposed to the water motion requires the stability of the top layer. For this, the Shields criterion is used; namely, the Shields parameter calculated for the top-layer stones must be smaller than the critical value of the Shields parameter corresponding to the initiation of motion (see, e.g., Sumer and Fredsøe, 2002).

Although a substantial amount of knowledge on the stability of rock berms had accumulated over the years, this is not the case when these structures are exposed to the motion of liquefied soil. Sumer et al. (2011) have conducted laboratory experiments to study the detailed mechanism of stability of such rock berms exposed to the orbital motion of liquefied soil. The present chapter essentially summarizes the results of this latter work.

The following two special tests carried out by Sumer et al. (2011) are particularly interesting. In order to compare the response of the berm structure, Sumer et al. (2011) carried out two tests: (1) when the structure was exposed to water; and (2) when it was exposed to liquefied soil. In the first test, the berm structure was placed in position in the sediment box without the sediment, and it was exposed to water in the test. In the second test, the berm structure was placed in the sediment box with the sediment present, and therefore the berm structure was, upon liquefaction of the sediment, exposed to the orbital motion of the liquefied sediment. The berm material was round stones the size 2.5 cm. The berm structure was exactly the same in both experiments. The wave climate was also exactly the same in the two tests, with the wave height $H = 17$ cm, the wave period $T = 1.6$ s and the water depth $h = 40$ cm. The amplitude of the orbital velocity of water particles in the first test, and that of liquefied-soil particles in the second test were measured as function of the vertical distance. Although the orbital velocity in the water test is a factor of 7 larger than in the case of the liquefied soil, stones did not move at all in the water experiment, and the berm structure remained completely intact, while a fairly substantial amount of damage occurred in the case of the liquefied soil. Sumer et al. (2011) checked for the incipient motion in the water case, and found that the Shields parameter was smaller than the critical value for the initiation of the motion, and therefore the stones should not move in the water case, as revealed in the test.

The question is why the same stones under the same setting and under the same wave climate (with even a factor of 7 smaller orbital velocity magnitude) move in the case of the liquefied sediment. Sumer et al. (2011) listed the following factors contributing to the ”earlier” incipient stone motion in the case of the liquefied soil: (1) The stones are lighter in the liquefied soil by a factor of 2.3 than in water; (2) This implies that the friction force is a factor of 2 less in the liquefied soil; (3) The drag coefficient in liquefied soils is 8 orders of magnitude larger than the water values; and (4) The inertia force is also larger in liquefied soil than in water.

As noted in the preceding paragraphs, stones of a berm structure which cannot be moved in water can easily be moved in liquefied soil under the same waves.

The degree of the stone movement (i.e., the damage) in the latter case could be fairly substantial and therefore the berm needs to be designed to ensure its stability if and when the soil is liquefied. Sumer et al. (2011) described the initiation of stone motion as function of three governing parameters, namely, the mobility number, the Keulegan-Carpenter number, and the Reynolds number. Figure 9 is reproduced from Sumer et al. (2011) in which Ψ is the mobility parameter,

$$\Psi = \frac{U_m^{\ 2}}{g(\frac{\rho_s}{\rho_{liq}} - 1)D} \tag{15}$$

KC is the Keulegan-Carpenter number,

$$KC = \frac{U_m T}{D} \tag{16}$$

and Re_D is the Reynolds number,

$$\mathrm{Re}_D = \frac{DU_m}{\nu'} \tag{17}$$

in which D is the stone size, U_m is the amplitude of the orbital velocity of liquefied soil in the undisturbed case at the level of the top of the berm, g is the acceleration due to gravity, T is the wave period, ρ_s is the density of soil grains, ρ_{liq} is the density of the liquefied soil, ν' is the kinematic viscosity of the liquefied soil, calculated from $\nu' = [2/(2-3c)]\nu$ with ν being the kinematic viscosity of water, and c the solid concentration (volume concentration) of liquefied soil.

The specific gravity of the liquefied soil, ρ_{liq}/ρ can be taken as 1.93, and the concentration c can be worked out from

$$\frac{\rho_{liq}}{\rho} = (1-c) + c\frac{\rho_s}{\rho} \tag{18}$$

As Sumer et al. (2011) pointed out, the size of the data in Figure 9 is too small to resolve the KC dependence of the critical mobility number for the range of the Keulegan-Carpenter number encountered in practice, namely $KC < O(40)$. However, the diagram can, to a first approximation, be used when KC remains within the range tested in the experiments. Sumer et al. (2011) also note that the mobility-number data did not give any marked trend when plotted as function of the Reynolds number. The real-life situations may involve Reynolds numbers large compared with the

Reynolds numbers in Figure 9. Therefore caution must be exercised when extending the results in Figure 9 to prototype conditions. See the discussion under Remarks on Practical Application in Sumer et al. (2011).

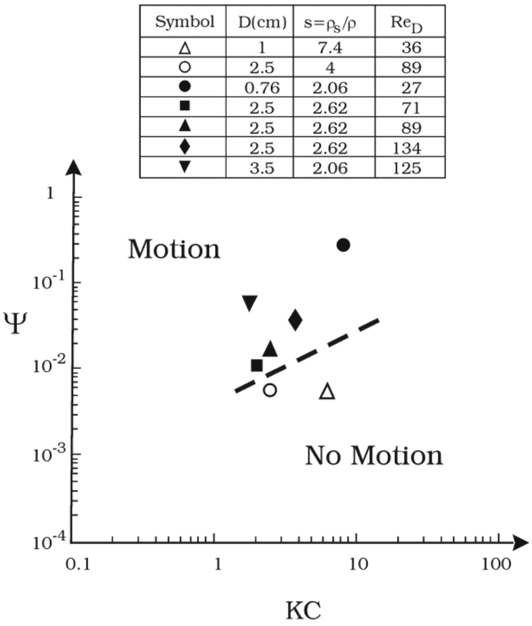

Figure 9 Incipient stone motion in liquefied soil. Filled symbols: Motion. Empty symbols: No motion. Sumer et al. (2011).

8. IMPACT OF SEISMIC-INDUCED LIQUEFACTION

Earthquakes are an open, direct threat to marine structures (such as quay walls, piers, dolphins, breakwaters, buried pipelines, sheet-piled structures, containers, silos, warehouses, storage tanks located in coastal areas, etc.) when structures are located at or near the epicenter. The structure in this case will be exposed to the devastating shaking effect of the seismic action, and the result can be catastrophic.

Earthquakes may also be a threat to marine structures in an indirect way, through the shaking of the supporting soil. The stability and integrity of structures will be at risk if the soil fails due to liquefaction as a result of the shaking of the soil. This kind of failure also can be catastrophic, as observed, for example, in the 1995 Japan Kobe earthquake, and the 1999 Turkey Kocaeli earthquake.

Liquefaction-induced damage to marine structures has been documented quite extensively in the literature: Wyllie et al. (1986) (Chile); Iai and Kameoka (1993) (Japan); Iai et al. (1994) (Japan); Hall (1995) (USA); Sugano et al. (1999) (Taiwan); Boulanger et al. (2000) (Turkey); Sumer et al. (2002) (Turkey); and Katopodi and Iosifidou (2004) (Greece), to give but a few examples. A partial list of well-documented case histories can be found in PIANC (2001).

An extensive review of the subject has been presented in a recent paper (Sumer et al., 2007). The contributors to the original publication (Sumer et al., 2007) according to the sections were as follows:

- Seismic-Induced Liquefaction by Professor Atilla Ansal;
- Review of the Existing Codes/Guidelines with Special Reference to Marine Structures by Dr. Niels-Erik Ottesen Hansen and Mr. Jesper Damgaard;
- Japanese Experience of Earthquake-Induced Liquefaction Damage on Marine Structures by Professor Kouki Zen;
- Turkey Kocaeli Earthquake and Liquefaction Damage on Marine Structures by Professor Ali Riza Gunbak, Professor Yalcin Yuksel, Dr. Niels-Erik Ottesen Hansen, Professor Adrzej Sawicki, and the author;
- Assessment of Liquefaction-Induced Lateral Ground Deformations by Professor K. Onder Cetin; and
- Tsunamis and Their Impacts by Professor Ahmet C. Yalciner and Professor Costas Synolakis.

The authors emphasize that their paper (Sumer et al., 2007) and the existing guidelines, namely (1) European Committee for Standardization (CEN), 1994, Eurocode 8: Design Provisions for Earthquake Resistance of Structures; (2) ASCE, 1998, Seismic Guidelines for Ports; and (3) PIANC, 2001, Seismic Design Guidelines for Port Structures, form a complementary source of information on the impact of seismic-induced liquefaction.

For detailed analyses, the reader is referred to Sumer et al. (2007) or Sumer (2014, Chapter 10) which is essentially extracted from Sumer et al. (2007).

9. ACKNOWLEDGEMENTS

The author would like to thank Dr. Shinji Sassa for inviting the author to prepare this paper. Support from MERMAID, a 7th Framework European Union project, is also acknowledged: Innovative Multi-purpose Offshore Platforms: Planning, Design and Operation (MERMAID), 2012-2016, Grant Agreement No. 288710 of European Commission, 7th Framework Programme for Research.

10. REFERENCES

ASCE (American Society of Civil Engineer) (1998): Seismic Guidelines for Ports. Written by the Ports Committee of the Technical Council on Lifetime Earthquake Engineering, Monograph No. 12. Ed. Stuart D. Werner, New York.

Barends, F.B.J. and Calle, E.O.F. (1985): A method to evaluate the geotechnical stability of off-shore structures founded on a loosely packed seabed sand in a wave loading environment. Behaviour of Offshore Structures, Elsevier Science Publishers B.V. Amsterdam, 643-652.

Boulanger, R., Iai, S., Ansal, A., Cetin, K.O., Idriss, I.M., Sunman, B. and Sunman, K. (2000): Performance of Waterfront Structures. 1999 Kocaeli, Turkey, Earthquake Reconnaissance Report, Chap. 13, Supplement A to Earthquake Spectra, vol. 16, T.L. Youd, J.-P. Bardet, J.D. Bray, eds., 295-310.

Brown, R.J. (1975): How to protect offshore pipelines. Pipeline Ind., vol. 42, No. 3, 43-47.

Chan, A.H.C. (1988): A Unified Finite-element Solution to Static and Dynamic Geomechanics Problems. Ph.D. Thesis, Univ. College of Swansea, Wales.

Chan, A.H.C. (1995): User Manual for DIANA-SWANDYNE II. Department of Civil Engineering, Univ. of Birmingham.

Chowdury, B., Dasari, G.R. and Nogami, T. (2006): Laboratory study of liquefaction due to wave-seabed interaction. J. Geotechnical and Geoenvironmental Eng., ASCE, vol. 132, No. 7, 842-851.

Coastal Engineering Manual (2006): Types and functions of coastal structures. Part VI, Chapter 2, Engineer Manual EM 1110-2-1100, Update: 1. June, 2006. Headquarters, U.S. Army Corps of Engineers, Washington, D.C.

Damgaard, J., Sumer, B.M., Teh, T.C., Palmer, A.C., Foray, P. and Osorio, D. (2006): Guidelines for pipeline on-bottom stability on liquefied noncohesive seabeds. J. Waterway, Port, Coastal and Ocean Engineering, ASCE, vol. 132, No. 4, 300-309.

de Groot, M.B., Lindenberg, J. and Meijers, P. (1991): Liquefaction of sand used for soil improvement in breakwater foundations. Proc. Int. Symp. Geo-coast’ 91, Yokohama, 555-560.

de Groot, M.B., Kudella, M., Meijers, P. and Oumeraci, H. (2006): Liquefaction Phenomena underneathMarine Gravity Structures Subjected to Wave Loads. J. Waterway, Port, Coastal and Ocean Engineering, ASCE, vol. 132, No. 4, 325-335.

de Rouck, J. (1991): De stabiliteit van storsteengolfbreakers. (Stability of rubble mound breakwaters. Slope stability analysis; a new armour unit). Dr. thesis, Dep. Burgerlijke Bouwkunde, Laboratorium voor hydraulica, Katholieke Univ. Leuven, Faculteit Toegepaste Wetenschapen, Leuven, Belgium.

de Rouck, J. and Troch, P. (2002). Pore water pressure response due to tides and waves based on prototype measurements. PIANC Bulletin No. 110, 9-31.

de Rouck, J. and van Damme, L. (1996): Overall stability analysis of rubble mound breakwaters. Proc. 25th Int. Conf. on Coastal Engineering, Orlando, Fla., ASCE, Reston, Va., 1603-1616.

Dunn, S.L., Vun, P.L., Chan, A.H.C. and Damgaard, J.S. (2006): Numerical modeling of wave-induced liquefaction around pipelines. J. Waterway, Port, Coastal, and Ocean Engineering, ASCE, vol 132, No. 4, 276-288.

European Committee for Standardization (CEN) (1994): Eurocode 8: Design Provisions for Earthquake Resistance of Structures, Part 1-1— General rules for structures (ENV-1998-1-1); Part 5—Formations, retaining structures and geotechnical aspects (ENV 1998-5).

Gratchev, I.B., Sasa, K., Osipov, V.I. and Sokolov V.N. (2006): The liquefaction of clayey soils under cyclic loading. Eng. Geology, vol. 86, 70-84.

Hall, J.F. (ed.) (1995): Northridge Earthquake of January 17, 1994. Reconnaissance Report, vol. 1, Earthquake Spectra, Supplement C to vol. 11.

Hattori, A., Sakai, T. and Hatanaka, K. (1992): Wave-induced porewater pressure and seabed stability. Proceedings of the 23rd Conference on Coastal Engineering (ICCE), vol. 2, 2095-2107.

Herbich, J.B. (1981): Offshore Pipeline Design Elements. Marcel Dekker, Inc., New York and Basel.

Hsu, J.R.S. and Jeng, D.S. (1994): Wave-Induced soil response in an unsaturated anisotropic seabed of finite thickness. International Journal for Numerical and Analytical Methods in Geomechanics, vol. 18, 785-807.

Iai, S. and Kameoka, T. (1993): Finite element analysis of earthquake induced damage to anchored sheet pile quay walls. Soils and Foundations, vol. 33, No. 1, 1, 71-91.

Iai, S., Matsunaga, Y., Morita, T., Miyata, M., Sakurai, H., Oishi, H., Ogura, H., Ando, Y., Tanaka, Y and Kato, M. (1994): Effects of remedial measures against liquefaction at 1993 Kushiro-Oki earthquake. Proc. 5th US-Japan Workshop on Earthquake Resistant Design of Lifeline Facilities and Counter Measures against Soil Liquefaction, NCEER-94-0026, National Center for Earthquake Engineering Research, 135-152, Buffalo, N.Y.

Idriss, I.M. and Boulanger, R.W. (2008): Soil Liquefaction During Earthquakes. Earthquake Engineering Research Institute, Oakland, CA, 244 p.

Jefferies, M. and Been, K. (2006): Soil Liquefaction. A Critical State Approach. Taylor & Francis, 479 p.

Jeng, D.-S. (2013): Porous Models for Wave-seabed Interactions. Shanghai Jiao Tong University Press and Springer Heidelberg, New York, Dordrecht, London.

Jeng, D.S. and Seymour, B.R. (2007): Simplified analytical approximation for pore-water pressure buildup in marine sediments. J.Waterway, Port, Coastal, and Ocean Engineering, ASCE, vol 133, No. 4, 309-312.

Jeng, D.S, Seymour, B.R. and Li, J. (2007): A new approximation for pore pressure accumulation in marine sediment due to water waves. International J. for Numerical and Analytical Methods in Geomechanics, vol. 31, 53-69.

Jeng, D.S., Ye, J.H., Zhang, J.-S. and Liu, P.L.F. (2013): An integrated model for the wave-induced seabed response around marine structures: Model verifications and applications. Coastal Engineering, vol. 72, 1-19.

Katopodi, I. and Iosifidou, K. (2004): Impact of the Lefkada earthquake (14-08-2003) on marine works and coastal regions, Proc., 7th Panhellenic Geographical Conference, Mytilene, Greece, October 2004, 363-370.

Kirca, V.S.O. (2013): Sinking of irregular shape blocks into marine seabed under wave-induced liquefaction. Coastal Engineering, vol. 75, 40–51.

Kirca, V.S.O., Sumer, B.M. and Fredsøe, J. (2013): Seabed liquefaction under standing waves. Journal of Waterway, Port, Coastal and Ocean Engineering, ASCE. vol. 139, No. 6, 489–501.

Kirca, V.S.O., Sumer, B.M. and Fredsoe, J. (2014): Influence of clay content on wave-induced liquefaction. Journal of Waterway, Port, Coastal, and Ocean Engineering, ASCE. In print.

Kramer, S.L. (1996): Geotechnical Earthquake Engineering. Prentice Hall, 653 p.

Kudella, M., Oumeraci, H., de Groot, M.B., and Meijers, P. (2006): Large-scale experiments on pore pressure generation underneath a caisson breakwater. J. Waterway, Port, Coastal and Ocean Engineering, ASCE, vol. 132, No. 4, 310-324.

Maeno, S. and Nago, H. (1988): Settlement of a concrete block into a sand bed under water pressure variation. Modelling Soil-Water-Structure Interactions. Kolkman et al. (eds.), 67-76, Balkema, Rotterdam, The Netherlands.

Maeno, S., Magda, W. and Nago, H. (1999): Floatation of buried pipeline under cyclic loading of water pressure. Proceedings of the 9th International Offshore and Polar Engineering Conference and Exhibition, Brest, France, May 30- June 4, 1999, vol. II, 217-225.

McDougal, W.G., Tsai, Y.T., Liu, P.L-F. and Clukey, E.C. (1989): Wave-induced pore water pressure accumulation in marine soils. Journal of Offshore Mechanics and Arctic Engineering, ASME, vol. 111, No. 1, 1–11.

Mei, C.C. and Foda, M.A. (1981): Wave-induced responses in a fluid filled poroelastic solid with a free surface A boundary layer theory. Geophysics, Journal of the Royal Astronomical Society, vol. 66, No. 3, 597–631.

Michallet, H., Mory, M., and Piedra-Cueva, I. (2009): Wave-induced pore pressure measurements near a coastal structures, Journal of Geophysical Research, vol. 114, No. C06019, 1–18.

Michallet, H., Rameliarison, V., Berni, C., Bergonzoli, M., Barnoud, J.-M. and Barthelemy, E. (2012 a): Physical modelling of sand liquefaction under wave breaking on a vertical wall. 33rd Conference on Coastal Engineering, Santander, Spain, ICCE 2012, July 1–6, 2012.

Michallet, H., Catalano, E., Berni, C., Chareyre, B., Rameliarison, V. and Barthelemy, E. (2012 b): Physical and numerical modelling of sand liquefaction in waves interacting with a vertical wall. 6th International Conference on Scour and Erosion (ICSE6), August 27–31, 2012, Paris, 679–686.

Miyamoto, J., Sassa, S. and Sekiguchi, H. (2003): Preshearing effect on the wave-induced liquefaction in sand beds. Proc. Soil and Rock America, Boston, US, vol. 1, 1025-1032.

Miyamoto, J., Sassa, S. and Sekiguchi, H. (2004): Progressive solidification of a liquefied sand layer during continued wave loading. Geotechnique, vol. 54, No. 10, 617-629.

Mory, M., Michallet, H., Bonjean, D., Piedra-Cueva, I., Barnoud, J.M., Foray, P., Abadie, S. and Breul P. (2007): A field study of momentary liquefaction caused by waves around a coastal structure. Journal of Waterway, Port, Coastal and Ocean Engineering, ASCE, vol. 133, No. 1, 28-38.

PIANC (2001): Seismic Design Guidelines for Port Structures. Working Group No. 34 of the Maritime Navigation Commission, International Navigation Association (PIANC). A.A. Balkema Publishers.

Powrie, W. (2002): Soil Mechanics. 2nd edition. Spon Press, Taylor and Francis Group, London, x+675p.

Rahman, M.S., Seed, H.B. and Booker, J.R. (1977): Pore pressure development under offshore gravity structures. J. Geotechnical Eng. Division, ASCE, vol. 103, No. GT12, 1419-1436.

Sakai, T., Hatanaka, K. and Mase, H. (1992 a): Wave-induced effective stress in seabed and its momentary liquefaction. J. Waterway, Port, Coastal and Ocean Engineering, ASCE, vol. 118, No. 2, 202-206. See also Discussions and Closure in vol. 119, No. 6, 692-697.

Sakai, T., Mase, H., Cox, D.T. and Ueda, Y. (1992 b): Field observation of wave-induced porewater pressures. Proceedings of the 23rd Conference on Coastal Engineering (ICCE), vol. 2, 2397-2410.

Sakai, T., Gotoh, H. and Yamamoto, T. (1994): Block subsidence under pressure and flow. Proc. 24th Conference on Coastal Engineering (ICCE 94), 23-28. October, 1994, Kobe, Japan, 1541-1552.

Sandven, R., Foray, P. and Long, M. (2004): Review of test methods for evaluation of liquefaction potential, with special emphasis on wave induced liquefaction and determination of air/gas content. Project Report, EU LIMAS Project EVK3-CT-2000_00038. Final review report, revision date: 20045.04.30. NTNU Geotechnical Division, Trondheim, Norway. April 2004. Electronic copy obtainable from B. Mutlu Sumer.

Sandven, R., Husby, E., Husby, J.E., Jønland, J., Roksvåg, K.O., Staehli, F. and Tellugen, R. (2007): Development of a sampler for measurement of gas content in soils. Journal of Waterway, Port, Coastal and Ocean Engineering, ASCE, vol. 133, No. 1, 3-13.

Sassa, S. and Sekiguchi, H. (1999): Wave-induced liquefaction of beds of sand in a centrifuge. Geotechnique, vol. 49, No. 5, 621-638.

Sassa, S. and Sekiguchi, H. (2001): Analysis of wave-induced liquefaction of sand beds. Geotechnique, vol. 51, No. 2, 115-126.

Schlichting H. (1979): Boundary-Layer Theory. McGraw-Hill.

Schofield, A.N. (1980): Cambridge geotechnical centrifuge operations. Geotechnique, vol. 30, No. 3, 227-268.

Seed, H.B. and Idriss, I.M. (1982): Ground Motions and Soil Liquefaction During Earthquakes. Earthquake Engineering Research Institute, Oakland, CA, 134 p.

Seed, H.B. and Rahman, M.S. (1978): Wave-induced pore pressure in relation to ocean floor stability of cohesionless soil. Marine Geotechnology, 3, No. 2, 123-150.

Sekiguchi, H. and Phillips, R. (1991): Generation of water waves in a drum centrifuge. Proc. Int. Conf. CENTRIFUGE 91, Boulder, USA, 343-350.

Sekiguchi, H., Kita, K. and Okamoto, O. (1995): Response of poroelastoplastic beds to standing waves. Soils and Foundations, vol. 35, No. 3, 31-42, Japanese Geotechnical Society.

Sekiguchi, H., Kita, K., Sassa, S. and Shimamura, T. (1998): Generation of progressive fluid waves in a geo-centrifuge. Geotech. Test. J., vol. 21, No. 2, 95-101.

Sekiguchi, H., Sassa, S., Sugioka, K. and Miyamoto, J. (2000): Waveinduced liquefaction, flow deformation and particle transport in sand beds. Proc. Int. Conf. GeoEng2000, Melbourne, Australia, Paper No. EG-0121.

Sills, G., Wheeler, S.J., Thomas, S.D. and Gardner, T.N. (1991): Behaviour of offshore soils containing gas bubbles. Geotechnique, vol. 41, No. 2, 227–241.

Spierenburg, S.E.J. (1987): Seabed Response to Water Waves. Ph. D. dissertation, Delft University of Technology, The Netherlands.

Sugano, T., Kaneko, H. and Yamamoto, S. (1999): Damage to port facilities. The 1999 Ji-Ji Earthquake, Taiwan. Investigation into the Damage to Civil Engineering Structures, Japan Society of Civil Engineers, 5-1–5-7.

Sumer, B.M. (2006): Special issue on liquefaction around marine structures: Processes and benchmark cases. Journal of Waterway, Port, Coastal and Ocean Engineering, ASCE, vol. 132, No. 4, 225–226.

Sumer, B.M. (2007): Special issue on liquefaction around marine structures: Miscellaneous. Journal of Waterway, Port, Coastal and Ocean Engineering, ASCE, vol. 133, No. 1, 1–2.

Sumer, B.M. (2014): Liquefaction Around Marine Structures. World Scientific. Singapore.

Sumer, B.M. and Cheng, N.-S. (1999): A random-walk model for pore pressure accumulation in marine soils. Proceedings of the 9th International Offshore and Polar Engineering Conference, ISOPE-99, Brest, France, 30 May–4 June, 1999, vol. 1, 521–526.

Sumer, B.M. and Fredsoe, J. (2002): The Mechanics of Scour in the Marine Environment. World Scientific, Singapore, 552 p.

Sumer, B.M., Fredsøe, J., Christensen, S. and Lind, M.T. (1999): Sinking/Floatation of pipelines and other objects in liquefied soil under waves. Coastal Engineering, vol. 38, No. 2, 53–90.

Sumer, B.M., Whitehouse, R.J.S. and Tørum, A. (2001): Scour around coastal structures: A summary of recent research. Coastal Engineering, Vol. 44, No. 2, 153–190.

Sumer, B.M., Kaya, A. and Hansen, N.-E.O. (2002): Impact of liquefaction on coastal structures in the 1999 Kocaeli, Turkey Earthquake. Proceedings of the 12th International Offshore and Polar Engineering Conference, KitaKyushu, Japan, May 26–31, 2002, vol. II, 504–511.

Sumer, B.M., Hatipoglu, F. and Fredsoe, J. (2004): The cycle of soil behaviour during wave liquefaction, Book of Abstracts, Paper 171, 29th International Conference on Coastal Engineering, 19–24 September, 2004, National Civil Engineering Laboratory (LNEC), Lisbon, Portugal.

Sumer, B.M., Hatipoglu, F., Fredsoe, J. and Sumer, S.K. (2006 a): The sequence of soil behaviour during wave-induced liquefaction. Sedimentology, vol. 53, 611–629.

Sumer, B.M., Hatipoglu, F., Fredsoe, J. and Hansen, N.-E.O. (2006 b): Critical floatation density of pipelines in soils liquefied by waves and density of liquefied soils. Journal of Waterway, Port, Coastal and Ocean Engineering, ASCE, vol. 132, No. 4, 252–265.

Sumer, B.M., Ansal, A., Cetin, K.O., Damgaard, J., Gunbak, A.R., Hansen, N.-E.O., Sawicki, A., Synolakis, C.E., Yalciner, A.C., Yuksel, Y. and Zen, K. (2007): Earthquake-induced liquefaction around marine structures. Journal ofWaterway, Port, Coastal and Ocean Engineering, ASCE, vol. 133, No. 1, 55–82.

Sumer, S.K., Sumer, B.M., Dixen, F.H. and Fredsøe, J. (2008): Pore pressure buildup in the subsoil under a caisson breakwater. Proceedings of the 18th International Offshore (Ocean) and Polar Engineering Conference, ISOPE 2008, Vancouver, BC, Canada, July 6–11, 664–671.

Sumer, B.M., Dixen, F.H. and Fredsøe, J. (2010): Cover stones on liquefiable soil bed under waves. Coastal Engineering, vol. 57, No. 9, 864–873

Sumer, B.M., Dixen F.H. and Fredsoe, J. (2011): Stability of submerged rock berms exposed to motion of liquefied soil in waves. Ocean Engineering. vol. 38, No. 7, 849–859.

Sumer, B.M., Kirca, V.S.O. and Fredsoe, J. (2012): Experimental validation of a mathematical model for seabed liquefaction under waves. International Journal of Offshore and Polar Engineering, vol. 22, No. 2, June 2012, 133–141.

Taylor, R.N. (1995): Centrifuge in modelling: principles and scaling effects. In: Geotechnical Centrifuge Technology. Blackie Academic & Professional, London, 19–33.

Teh, T.C., Palmer, A. and Damgaard, J. (2003): Experimental study of marine pipelines on unstable and liquefied seabed. Coastal Engineering, vol. 50, No. 1–2, 1–17.

Teh, T.C., Palmer, A., Bolton, M.D. and Damgaard J. (2006): Stability of submarine pipelines on liquefied seabeds. Journal

Waterway, Port, Coastal and Ocean Engineering, ASCE, vol. 132, No. 4, 244–251.
Tørum, A. (2007): Wave-induced pore pressures–Air/gas content. Journal of Waterway, Port, Coastal and Ocean Engineering, ASCE, vol. 133, No. 1, 83–86.
Wyllie, L.A., Abrahamson, N., Bolt, B., Castro, G., Durkin, M.E., Escalante, L., Gates, H.J., Luft, R., McCormic, D., Olson, R.S., Smith, P.D. and Vallenas, J. (1986): The Chile earthquake of March 3, 1985. Earthquake Spectra, vol. 2, No. 2, 293–371.
Yamamoto, T., Koning, H.L., Sellmeijer, H. and van Hijum, E. (1978): On the response of a poro-elastic bed to water waves. Journal of Fluid Mechanics, vol. 87, No. 1, 193–206.
Zen, K. and Yamazaki, H. (1990 a): Mechanism of wave-induced liquefaction and densification in seabed. Soils and Foundations, vol. 30, No. 4, 90–104.
Zen, K. and Yamazaki, H. (1990 b): Oscillatory pore pressure and liquefaction in seabed induced by ocean waves. Soils and Foundations, vol. 30, No. 4, 147–161.
Zienkiewicz, O.C., Chan, A.H.C., Pastor, M., Paul, D.K. and Shiomi, T. (1990): Static and dynamic behaviour of geomaterials — A rational approach to quantitative solutions. Part I: Fully saturated problems. Proceedings of the Royal Society of London, Series A, vol. 429, 285–309.
Zienkiewicz, O.C., Chan, A.H.C., Pastor, M., Schrefler, B.A. and Shiomi, T. (1999): Computational Geomechanics with Special Reference to Earthquake Engineering. Wiley, Chichester, U.K.